Novel Diazamesocyclic Ligands Functionalized with Pyridyl Donor Group(s) − Synthesis, Crystal Structures, and Properties of Their Copper(II) Complexes

Xian-He Bu,*[a] Miao Du,[a] Zhi-Liang Shang,[a] Lei Zhang,[a] Qi-Hua Zhao,[a]
Ruo-Hua Zhang,[b] and Mitsuhiko Shionoya[c]

Keywords: Diazamesocyclic ligands / Copper(II) complexes / Crystal structures / Magnetic properties

Two novel diazamesocyclic ligands based on 1,5-diazacyclooctane (DACO) and functionalized with additional pyridyl donor groups, namely 1,5-bis(2-pyridylmethyl)-1,5-diazacyclooctane (**L^1**) and 1-(2-pyridylmethyl)-1,5-diazacyclooctane (**L^2**), have been synthesized and characterized, as have their Cu^{II} complexes. Crystal structure analyses revealed that with Cu(ClO$_4$)$_2$ **L^1** forms a five-coordinate mononuclear complex [Cu^{II}**L^1**Cl]ClO$_4$ (**1**), whereas **L^2** forms a μ-Cl$^-$-bridged dinuclear complex [Cu^{II}(**L^2**)Cl]$_2$(ClO$_4$)$_2$ (**2**). Furthermore, it has been found that the apical chloride anion of **1** may be easily exchanged by azide anion, forming the mononuclear complex [Cu^{II}**L^1**(N$_3$)]ClO$_4$ (**3**). There is a notable difference between **3** and **1** in that **3** forms a quasi-two-dimensional network through intermolecular C–H···O hydrogen bonds and π–π stacking interactions. Each Cu^{II} center in the three complexes is pentacoordinated in a distorted square-pyramidal environment and the DACO ring of each ligand adopts a boat-chair configuration in all the complexes. In the mononuclear complexes **1** and **3**, the Cl$^-$ or N$_3$$^-$ anions occupy the apical sites, whereas in the dinuclear complex **2** the two bridging Cl$^-$ anions occupy both axial positions as well as one equatorial position, leading to an intramolecular Cu···Cu separation of 3.396 Å. Variable-temperature magnetic susceptibility measurements on **2** in the range 4–300 K indicate a weak intramolecular ferromagnetic coupling between adjacent Cu^{II} centers with $2J = 2.28$ cm^{-1}; the magneto-structural correlations are discussed in detail. The solution behavior of the complexes has been further studied by UV/vis and ESR techniques.

Introduction

Macrocyclic polyamines bearing functional groups and transition metal complexes thereof have been extensively studied in order to investigate the effects of the functional pendants on the coordination modes and properties of these complexes.[1] Mesocyclic diamines such as 1,5-diazacyclooctane (DACO), functionalized with pendant groups, can form stable metal complexes with unique conformational requirements,[2,3] and the coordinating abilities of such ligands can be adjusted through altering the donor groups on their skeletons.[4] This interesting chemistry prompted our investigation of DACO, in which we introduced functional donor groups on its backbone and examined the coordinating functionality of various pendant donors in relation to the structures and properties of the relevant metal complexes. Furthermore, the study of DACO derivatives and their metal complexes has been an active area of research owing to their use in analytical and biomimetic applications, in the stabilization of high oxidation states of some metal ions, in selective ion recognition, and as a result of their catalytic activities.[5]

Dinuclear Cu^{II} complexes play an important role in the elucidation of spin-coupling or magnetic-exchange phenomena between paramagnetic metal centers. They exemplify the simplest case where two unpaired electrons on two paramagnetic ions are separated by spacer ligands that may intramolecularly mediate the stabilization of a singlet. Several experimental and theoretical investigations have been carried out aimed at elucidating the structures and magnetic properties of bis(μ-chloro)-bridged Cu^{II} dimers, and different magnetic behavior ranging from ferro- to antiferromagnetic interactions has been found in these systems.[6] However, great difficulties remain in establishing a magneto-structural correlation for these complexes since they show pronounced Jahn−Teller distortion. Consequently, further investigations into the magneto-structural correlation of chloro-bridged Cu^{II} dinuclear complexes would seem necessary.

We report herein the synthesis of two new ligands based on DACO bearing one and two pyridine donor groups, respectively, as well as their Cu^{II} complexes (see Scheme 1). These tetra- and tridentate ligands form stable mononuclear and dinuclear complexes with Cu^{II}, the crystal structures of which have been elucidated by X-ray diffraction analysis. The magneto-structural correlations of **2** and the solution behavior of these Cu^{II} complexes have also been studied.

Results and Discussion

Syntheses and General Characterizations

The doubly-substituted ligand **L^1** was prepared by using an excess of 2-chloromethylpyridine hydrochloride, while an

---

[a] Department of Chemistry, Nankai University,
Tianjin 300071, P. R. China
Fax: (internat.) + 86-22/2353-0850
E-mail: buxh@nankai.edu.cn
[b] State Key Lab on Coordination Chemistry, Nanjing University,
Nanjing 210093, P. R. China
[c] Department of Chemistry, Graduate School of Science, The University of Tokyo,
Hongo, Tokyo 113−0033, Japan

1434−1948/01/0606−1551 $ 17.50+.50/0

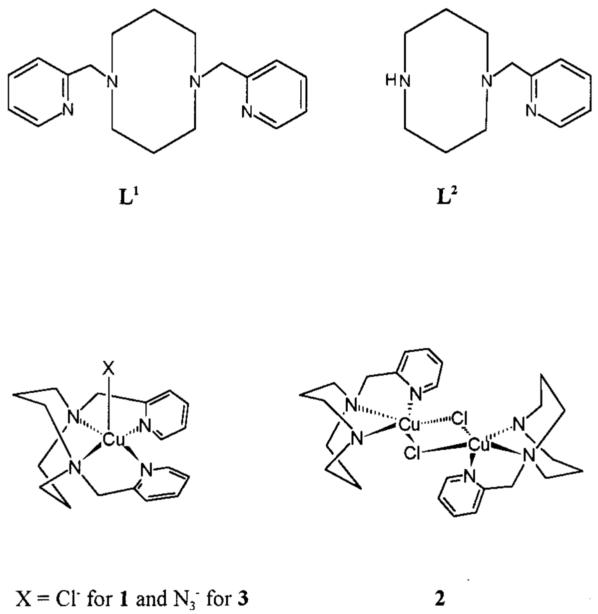

Scheme 1

excess of DACO was used to obtain the monoalkylated product **L**^{2}; both ligands were purified by column chromatography on silica gel. Acid-free **L**^{1} and **L**^{2} could only be obtained as oils, hence they were converted into their HCl salts to obtain crystalline solids. The yields of both syntheses were in excess of 65% and all analytical data were in good agreement with the theoretical requirements of the two ligands.

The syntheses of **1** and **2** were accomplished by reacting the respective ligands with $Cu(ClO_4)_2·6H_2O$. Since the ligands were handled as their HCl salts, they first had to be neutralized with aqueous NaOH solution prior to complexation. Electrical conductance values in methanol solution indicated that **1** and **3** behave as 1:1 electrolytes, while **2** acts as a 2:1 electrolyte,[7] these findings being consistent with the crystal structural analyses. The IR spectra of the three complexes show absorption bands resulting from the skeletal vibrations of the pyridine rings in the region 1400−1600 cm^{-1}. The absorption bands due to ClO_4^- appear at 1098−1082 and 623−621 cm^{-1} for all three complexes. In addition, **3** exhibits three strong absorption bands at 2125, 2031, and 1098 cm^{-1} due to the ν_{N-N} stretch of the apical azide anion.

X-ray Crystal Structures of Complexes 1−3

The crystal structure of **1** showing the atom numbering scheme is depicted in Figure 1. The structure consists of a discrete [Cu**L**^{1}Cl]$^+$ cation and a perchlorate anion. The Cu^{II} center is coordinated by two pyridine nitrogen atoms and a pair of nitrogen donors of the DACO ring. A chloride anion completes the coordination polyhedron around the central metal ion. The Cu^{II} ion is pentacoordinated (CuN_4Cl) and the coordination polyhedron can best be described as a distorted square-pyramid with the chloride anion occupying the axial position. The Cu^{II} ion lies 0.425 Å above the basal least-squares plane defined by N(1), N(2), N(16), and N(26), in the direction of the apical Cl(1) anion, and the dihedral angle between the two pyridine rings is 36.1°. The ligand adopts a typical boat/chair configuration and with the central Cu^{II} ion forms two five-membered coordination rings N(1)−C(10)−C(11)−N(16)−Cu and N(2)−C(20)−C(21)−N(26)−Cu, resulting in an N(1)−Cu−N(16) angle of 79.8° and an N(1)−Cu−N(16) angle of 84.5°.

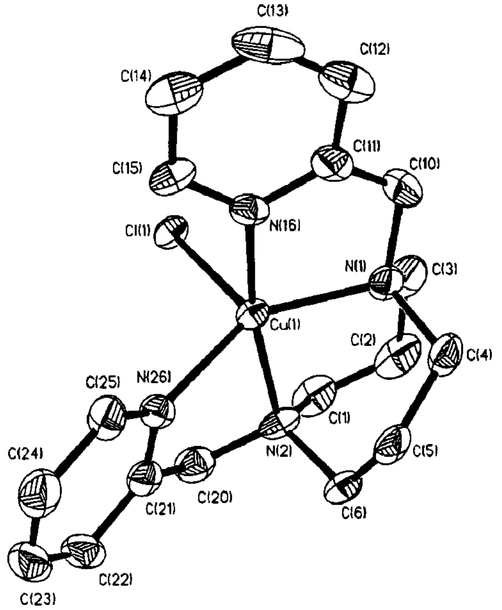

Figure 1. ORTEP view of **1** with thermal ellipsoids drawn at a 35% probability level

The two $Cu-N_{DACO}$ bond lengths are approximately equal (2.032 vs. 2.056 Å), both being normal Cu−N coordination bonds,[8] but the Cu−N(16) (pyridine) bond length is significantly shorter than the Cu−N(26) (pyridine) distance (1.991 vs. 2.113 Å), probably due to the steric interaction of the two pyridine groups.

The apical Cu−Cl(1) coordination bond measures 2.424 Å, which is close to the values reported for some similar complexes.[9,10] The weakly coordinated Cl$^-$ anion may be easily exchanged by other donor molecules or ions, hence the complex may have potential application in homogeneous catalysis or as a functional building block for the construction of larger functional architectures. We have successfully modified this complex by axial ligand exchange of chloride with azide, thereby generating **3**.

The crystal structure of **3** is shown in Figure 2(a); the coordination environment of the central Cu^{II} ion can be seen to be very similar to that in **1**. The Cu^{II} ion lies 0.424 Å above the mean basal plane defined by N(1), N(2), N(3), and N(4), in the direction of the apical N(5) atom. The dihedral angle between the two pendant pyridine rings is 27.7°, which is smaller than that in **1**, probably as a result of the less severe distortion of the coordination geometry about the central Cu^{II} ion. The $Cu-N_{DACO}$ bond lengths (2.041 vs. 2.075 Å) are close to the value found in **1** while, in contrast to **1**, the $Cu-N_{py}$ bond lengths are approximately the same (2.075 vs. 2.114 Å).

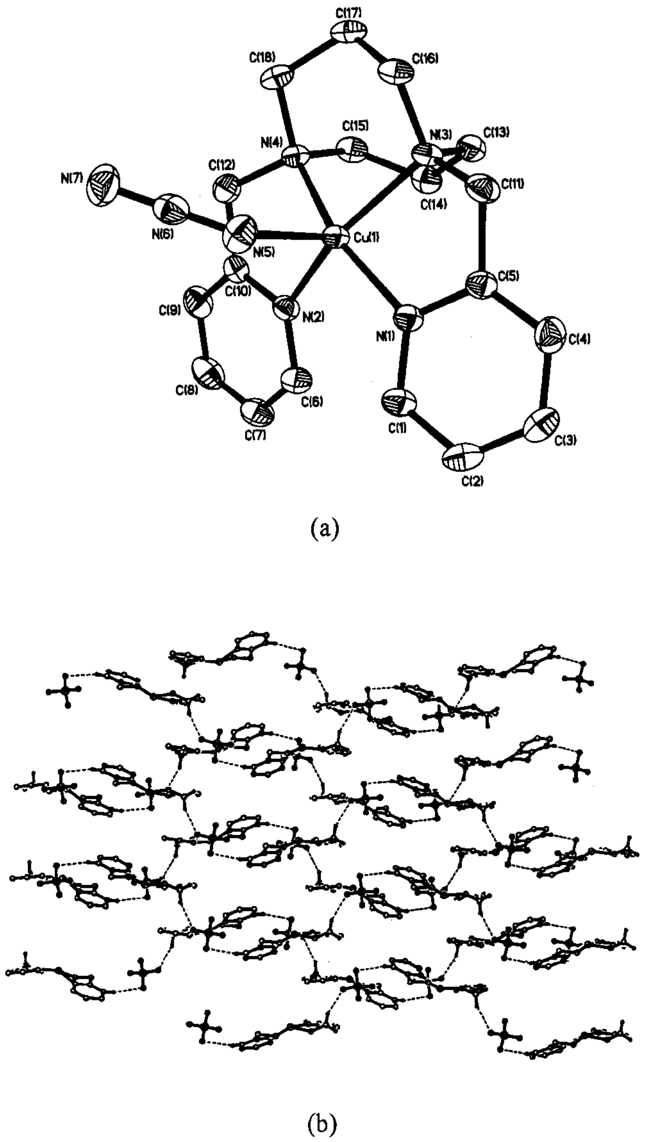

Figure 2. (a) ORTEP view of **3** with thermal ellipsoids drawn at a 30% probability level; (b) view of the two-dimensional network in **3** along the *b* axis; the methylene groups of the DACO ring and irrelevant hydrogen atoms have been omitted for clarity

Selected bond lengths and angles relevant to the Cu^{II} coordination spheres in both **1** and **3** are listed in Table 1. The stereo geometries of both of the five-coordinate (CuN_4X) complexes are distorted square-pyramids, as reflected in their τ values (0.38 and 0.29, respectively) defined by Addison et al. ($\tau = 0$ for an ideal square-pyramid, $\tau = 1$ for an ideal trigonal-bipyramid).[11] In both complexes, $\mathbf{L^1}$ acts as a tetradentate chelating agent. The coordination geometry around Cu^{II} is made up by a pair of nitrogen atoms of the DACO ring and the two nitrogen donors of the pyridine pendants, which occupy *cis* positions in the coordination polyhedron. In both complexes, the DACO ring of the ligand adopts a "boat/chair" configuration and is bent such that the central methylene C−H group of the boat form of the metalladiazacyclohexane ring shields the metal center with a H···Cu distance of 2.565 Å in **1** (2.555 Å in **3**) and a H−Cu−apex angle of 11.9° in **1** (7.9° in **3**). Thus, this methylene hydrogen effectively blocks the sixth coordination position, resulting in the observed five-coordinate metal complexes[4c] (see Scheme 2). The distances between the nitrogen atoms of the DACO ring are restricted to a narrow range with N_{DACO}−Cu−N'_{DACO} angles of 87.2° and 86.7° in the two complexes. The N_{py}−Cu−N'_{py} angles are also restricted within narrow limits (100.8° and 101.8°), due to the steric requirements of the ligand.

Table 1. Selected bond lengths [Å] and angles [°] in **1** and **3** (H* is the hydrogen of the central methylene group nearest to the Cu^{II} center in the boat forms of the metalladiazacyclohexane rings)

Complex **1**			
Cu−Cl(1)	2.424(2)	Cu−N(1)	2.056(7)
Cu−N(2)	2.032(6)	Cu−N(16)	1.991(6)
Cu−N(26)	2.113(6)	Cu···H*	2.565
N(2)−Cu(1)−N(16)	166.5(2)	N(1)−Cu(1)−N(26)	143.7(3)
N(1)−Cu(1)−N(2)	87.2(3)	N(16)−Cu(1)−N(26)	100.8(2)
N(2)−Cu(1)−N(26)	79.8(2)	N(1)−Cu(1)−N(16)	84.5(3)
H−Cu−apex	11.9		
Complex **3**			
Cu(1)−N(1)	2.025(2)	Cu(1)−N(4)	2.041(2)
Cu(1)−N(3)	2.075(2)	Cu(1)−N(5)	2.106(3)
Cu(1)−N(2)	2.114(2)	N(6)−N(7)	1.170(3)
N(6)−N(5)	1.174(3)	Cu···H*	2.555
N(1)−Cu(1)−N(3)	83.05(8)	N(4)−Cu(1)−N(2)	80.13(8)
N(4)−Cu(1)−N(3)	86.68(8)	N(1)−Cu(1)−N(2)	101.75(8)
N(3)−Cu(1)−N(2)	146.21(8)	N(1)−Cu(1)−N(4)	163.82(8)
N(7)−N(6)−N(5)	179.5(3)	H−Cu−apex	7.9

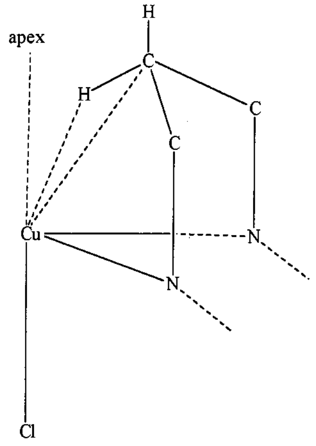

Scheme 2

The most notable difference between **3** and **1** is the ability of **3** to form a quasi-two-dimensional supramolecular network through weak intermolecular C−H···O hydrogen bonds and $\pi-\pi$ stacking interactions. This is illustrated in Figure 2(b). The hydrogen atoms of the pyridine ring and of the methylene group connected to the pyridine ring of another adjacent molecule in the cation unit $[CuL^1(N_3)]^+$ are activated by the positive charge that arises due to the coordination of the N atoms to the Cu^{II} center. Each perchlorate anion acts as a hydrogen-bond acceptor from two adjacent $[\mathrm{Cu}\mathbf{L}^1(\mathrm{N}_3)]^+$ cations, giving a one-dimensional infinite zigzag chain in the lattice. The C···O separations are 3.461 and 3.397 Å, with H···O separations of 2.561 and 2.484 Å. The C···O separations fall within the range of 3.0−4.0 Å suggested by Desiraju et al.,[12] while the bond angles of 161.5 and 163.4° are quite close to 180°. The Cu···Cu intermolecular distance between adjacent chains is 7.54 Å. Furthermore, the H-bonded chains are cross-linked in the unit cell. Two nearest pyridine planes, lying almost parallel to one another between the neighboring chains, show an average interfacial distance of 3.667 Å, indicating significant π-π stacking interactions.[13] As a result of these two types of weak intermolecular interaction, the $[\mathrm{Cu}\mathbf{L}^1(\mathrm{N}_3)]\mathrm{ClO}_4$ molecules are self-assembled into a quasi-two-dimensional network in this complex.

An ORTEP representation of **2**, showing the atom numbering scheme, is depicted in Figure 3, while selected bond lengths and angles are listed in Table 2. The complex consists of a discrete $[\mathrm{Cu}\mathbf{L}^2\mathrm{Cl}]_2^{2+}$ cation and two perchlorate anions. In the $[\mathrm{Cu}\mathbf{L}^2\mathrm{Cl}]_2^{2+}$ cation, the two Cu$^{\mathrm{II}}$ centers are symmetrically bridged by two chloride anions. Each Cu$^{\mathrm{II}}$ ion is bound by $\mathbf{L}^1$ through one nitrogen atom of the pyridyl pendant group and two nitrogen donors of the DACO ring, which again adopts a "boat/chair" configuration. The two bridging chloride anions complete the coordination polyhedron around each Cu$^{\mathrm{II}}$ ion. The Cu$^{\mathrm{II}}$ ions are pentacoordinated ($\mathrm{CuN_3Cl_2}$) and the coordination polyhedron around Cu$^{\mathrm{II}}$ may best be described as a distorted square-pyramid with $\tau = 0.34$.[11] The Cu$^{\mathrm{II}}$ ion lies 0.28 Å above the mean basal plane formed by N(1), N(2), N(11), and Cl(1a), in the direction of the apical Cl$^-$ anion, and the axial Cu(1)−Cl(1) distance is ca. 0.29 Å longer than the Cu(1)−Cl(1a) bond length in the basal plane (2.581 vs. 2.291 Å).

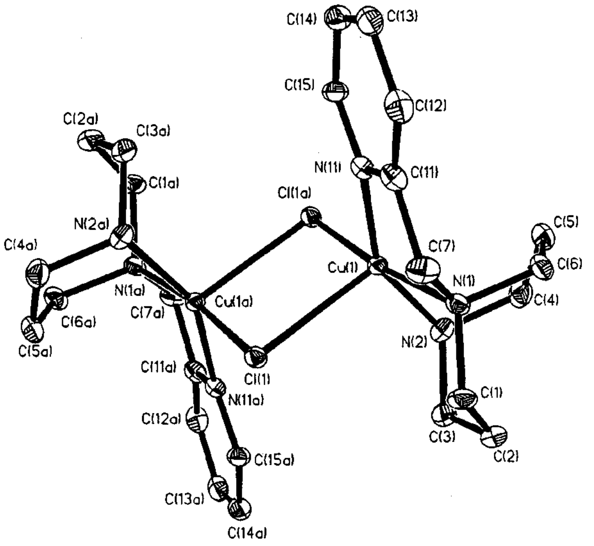

Figure 3. ORTEP representation of **2** with thermal ellipsoids drawn at a 35% probability level

The Cu$^{\mathrm{II}}$ centers and chloride anions form a rhombic plane with the angles Cl(1)−Cu(1)−Cl(1a) and Cu(1)−Cl(1)−Cu(1a) measuring 91.8° and 88.2°, respectively. The two intramolecular Cu$^{\mathrm{II}}$ centers in **2** have the same coordination configuration and structure. All the Cu−N and Cu−Cl bond lengths fall into the expected ranges for normal coordination bonds,[14] while the shortest Cu···Cu nonbonding length in the dimer is 3.396 Å.

Table 2. Selected bond lengths [Å] and angles [°] in **2**

Bond lengths [Å]			
Cu(1)−Cl(1)	2.581(1)	Cu(1)−N(1)	2.038(4)
Cu(1)−N(2)	2.007(5)	Cu(1)−N(11)	2.020(4)
Cu(1)−Cl(1a)	2.291(1)	Cu···H*	2.507
Bond angles [°]			
Cl(1)−Cu(1)−N(1)	95.2(1)	Cl(1)−Cu(1)−N(2)	105.3(1)
N(1)−Cu(1)−N(2)	86.5(2)	Cl(1)−Cu(1)−N(11)	100.4(1)
N(1)−Cu(1)−N(11)	82.2(2)	N(2)−Cu(1)−N(11)	152.7(2)
Cl(1)−Cu(1)−Cl(1a)	91.8(1)	N(1)−Cu(1)−Cl(1a)	173.0(1)
N(2)−Cu(1)−Cl(1a)	91.4(1)	N(11)−Cu(1)−Cl(1a)	96.8(1)
Cu(1)−Cl(1)−Cu(1a)	88.2(1)	H−Cu−apex	13.45

Electronic and ESR Spectra

The UV/vis spectra of the three complexes in methanol solution show absorption maxima at 621, 622, and 618 nm, respectively, which is in agreement with the absorptions seen for other five-coordinated Cu$^{\mathrm{II}}$ complexes with similar coordination geometries. The absorption bands of **1** and **2** display a slightly higher λ_{max} than that of **3**, suggesting that their coordination geometries are more distorted toward trigonal-bipyramid;[15] this is consistent with the degrees of distortion found in the X-ray structural analyses. This spectral feature is typical of pentacoordinated Cu$^{\mathrm{II}}$ complexes with distorted square-pyramidal geometry, which generally exhibit a band in the 550−660 nm range (d_{xz}, $\mathrm{d}_{yz} \rightarrow \mathrm{d}_{x^2-y^2}$).[15,16] In addition, the electronic spectra of all the complexes feature a characteristic absorption at about 260 nm attributable to a ligand $\pi \rightarrow \pi^*$ transition.

The X-band ESR spectra of **1** were measured in the polycrystalline state and in methanol solution, at room temperature and at 110 K. The following ESR parameters were obtained for polycrystalline powdered **1** at room temperature: $g_z = 2.21$, $g_y = 2.10$, and $g_x = 2.04$. The resolution did not improve very much upon cooling to 110 K, with parameters of $g_z = 2.26$, $g_y = 2.15$, and $g_x = 2.09$. Nevertheless, the spectra at 110 K did show some small splitting lines, probably due to the hyperfine splitting of the coordinated nitrogen donors. The g values conform to the relationship: $g_{\parallel} > g_{\perp} > g_{\mathrm{e}}$, which indicates that the unpaired 3d electron of the Cu$^{\mathrm{II}}$ ion should occupy the $\mathrm{d}_{x^2-y^2}$ orbital and a predominantly tetragonal component in the solid-state stereochemistry.[17] The different values of g_x and g_y for **1** imply that the Cu$^{\mathrm{II}}$ ground-state wavefunction is not pure $\mathrm{d}_{x^2-y^2}$, but that it contains some contribution from d_{z^2} as a result of the decreased symmetry of the coordination polyhedron, which is consistent with the crystal structure data. The room-temperature solution spectra show hyperfine splitting lines characteristic of Cu$^{\mathrm{II}}$ complexes, as was also observed for a frozen solution of **1**. The approximate

ESR parameters obtained were: $g_{\text{iso}} = 2.11$ ($A_{\text{iso}} = 74$ G), $g_{\|} = 2.23$ ($A_{\|} = 94$ G), and $g_{\perp} = 2.05$ ($A_{\perp} = 64$ G), where $g_{\perp} = (3g_{\text{iso}} - g_{\|})/2$ and $A_{\perp} = (3A_{\text{iso}} - A_{\|})/2$.[18] The values again conform to the relationship $g_{\|} > g_{\perp} > g_e$, with a smaller $A_{\|}$ value, indicating some distortion of the coordination geometry about the Cu$^{\text{II}}$ center from square-pyramidal in solution,[19] which is similar to the geometry observed in the solid state.

The X-band ESR spectrum of **2** in the solid state at room temperature shows isotropic character with $g_{\text{av}} = 2.10$, possibly as a result of exchange narrowing. No absorption is observed at half-field ($\Delta m_s = 2$, $g = 4$), indicating a small ZFS effect.[20] The spectrum of a frozen solution of **2** in methanol likewise exhibits only a quasi-isotropic feature, and the g value (2.10) is essentially the same as that of the polycrystalline sample. This indicates that there is no significant change in the coordination environment under the two sets of conditions.

Magnetic Properties

The magnetic behavior of **2** is shown in Figure 4 as the variation of χ_M (μ_{eff}) versus temperature. The molar magnetic susceptibility of the dinuclear Cu$^{\text{II}}$ unit increases with decreasing temperature. However, the effective magnetic moment increases very smoothly on lowering the temperature down to 14 K and finally decreases rapidly at even lower temperatures. This behavior indicates the existence of an intradimer *ferromagnetic exchange interaction*. The experimental data were least-squares fitted to the analytical expression given as Equation (1), according to the modified Bleaney−Bowers model for a Cu$^{\text{II}}$ dimer.[21] Here, all the symbols have their usual meanings; ρ is the percentage of non-coupled impurity and $N\alpha$ is the temperature-independent paramagnetism. The following parameters were obtained: $2J = 2.28$ cm^{-1}, $\rho = 0.005$, and $g = 2.12$, which is in good agreement with the average g value deduced from the ESR spectra. The agreement factor R [defined as $\Sigma(\chi_{\text{obs}} - \chi_{\text{calc}})^2/\Sigma(\chi_{\text{obs}})^2$] is equal to 2.0×10^{-5}.

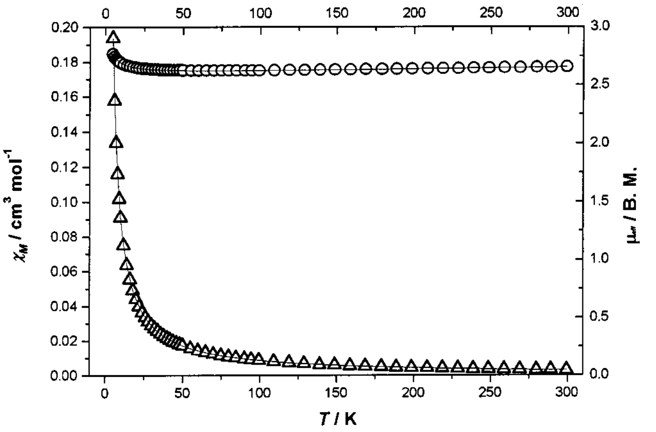

Figure 4. Magnetic coupling diagram of the μ-Cl$^-$-bridged binuclear complex **2**

$$\chi_M = (2Ng^2\beta^2/KT)[3 + \exp(-2J/KT)]^{-1}(1 - \rho) + Ng^2\beta^2\rho/2KT + N\alpha \quad (1)$$

In order to discuss the relationship between the magnitude of the exchange constant and the structural parameters in distorted square-pyramidal coordinated Cu$^{\text{II}}$ dimers with bis(μ-chloro) bridges, we have compiled the structural and magnetic parameters of several such Cu$^{\text{II}}$ dimers in Table 3.

In **2**, the spin density lies in the parallel planes and the magnetic orbital is almost orthogonal, indicating that the overlap is very small, and this leads to the observed weak magnetic exchange interaction. Hatfield and co-workers[22] have shown that antiferromagnetic interactions are observed when the value of the quotient φ/R (°/Å) is lower than 32.6 or higher than 34.8, whereas ferromagnetic interactions are observed for quotient values falling between these limits. For **2**, the quotient value is 34.17°, falling just within the aforementioned limits, hence the ferromagnetic interaction may be satisfactorily understood. In Cu$^{\text{II}}$ complexes, strict orthogonality does not occur,[23] and the ferromagnetic interaction is due to accidental orthogonality of the magnetic orbital involved and/or a polarization effect. In **2**, the π orbitals of the Cl(1) anion interact with the Cu(1) magnetic orbital; electron delocalization from the π orbital into the $d_{x^2-y^2}$ orbital of Cu(1) deposits some unpaired spin density of the same net orientation as that on Cu(1) onto the bridging Cl(1) anion. Therefore, coupling of the unpaired spins in the orthogonal orbitals, π and $d_{x^2-y^2}$ of Cu(2), leads to the triplet ground state.[24] According to the equation $J = J_F + J_{AF}$,[25] where $J_F = 2C$ and $J_{AF} = -2\Delta S$ (C is the two-electron exchange integral, S is the overlap integral, and Δ is the energy separation of the molecular magnetic orbital occupied by the unpaired electrons), J_F is the dominant term for **2**. It is worth noting that the Cu−Cl (equatorial) bond length is a key factor in

Table 3. The structural and magnetic properties of some bis(μ-Cl$^-$)-bridged Cu$^{\text{II}}$ dimeric complexes

Complex	Cu···Cu (Å)	Cu···Cl′ (R/Å)	Cu−Cl−Cu′ (φ/°)	φ/R (°/Å)	$2J$ (cm^{-1})	Ref.
[Cu(DMGH)Cl$_2$]$_2$	3.445	2.698	88.0	32.62	+6.3	14
[Cu$_2$(**L**^{2})$_2$Cl$_2$](ClO$_4$)$_2$	3.396	2.581	88.2	34.17	+2.24	this work
[Cu(Hfsaaep)Cl]$_2$	3.825	2.846	95.27	33.47	+0.3	6c
[Cu(TMSO)Cl$_2$]$_2$	3.737	3.020	88.5	29.30	−17.0	26
[Cu(TMEN)Cl$_2$]	4.089	3.147	96.8	30.76	−5.6	27
[Cu(2-pic)$_2$Cl$_2$]$_2$	4.404	3.364	100.63	29.91	−7.4	25, 28

determining the spin-polarization effect, which governs the magnitude of the magnetic exchange interaction.

Conclusion

The described synthetic procedure provides a convenient access to a new family of macrocyclic species and their metal complexes. The effect of substituents and of the apical anion on the five-coordinated Cu^{II} structural geometry is discussed in detail. A study of the magnetic properties has shown that the main structural factor determining the strength of the magnetic interaction is the value of the quotient (φ/R), but that the influence of the Cu−Cl equatorial and axial distances must also be considered.

Experimental Section

Materials and General Methods: The starting compound, DACO·2HBr, was prepared according to a literature method.[29,30] Other commercially available chemical reagents and solvents were of analytical grade and were purified by standard procedures prior to use. − FT-IR spectra were recorded on a Nicolet 170SX spectrometer at room temperature. − ^1H NMR spectra were recorded on a Bruker AC-P 200 spectrometer (200 MHz) at 25 °C using tetramethylsilane as an internal reference. − Electronic absorption spectra were recorded on a Hitachi UV-3010 spectrophotometer. − Elemental analyses were carried out on a Perkin−Elmer 240C analyzer. − Solution and polycrystalline EPR spectra (X-band) were recorded on a Bruker ER-200-DSRC10 spectrometer.

Syntheses of Ligands: 1,5-Bis(pyrid-2-ylmethyl)-1,5-diazacyclooctane Tetrahydrochloride Monohydrate (L^1·4HCl·H_2O): A suspension of DACO·2HBr (1.76 g, 6.4 mmol) and potassium hydroxide (0.73 g, 12.9 mmol) in anhydrous ethanol (40 mL) was stirred for 4 h at room temperature. A solution of 2-(chloromethyl)pyridine hydrochloride (2.46 g, 15.0 mmol) and triethylamine (2.09 g, 15.0 mmol) in anhydrous ethanol (20 mL) was then added dropwise to the stirred mixture over a period of 2 h. After the addition was complete, additional triethylamine (5 mL) was added and the resulting mixture was stirred for ca. two days at room temperature. The solvent was then removed under reduced pressure, the residue was redissolved in water (15 mL), and the pH of the resulting solution was adjusted to ca. 10 with anhydrous K_2CO_3. The organic phase that separated from the mixture was concentrated in vacuo and the crude product was purified by column chromatography on silica gel ($CH_2Cl_2/MeOH/NH_3·H_2O$, 10:10:1). The free ligand was obtained as a colorless oil; it was converted to its HCl salt, which was obtained as a white crystalline material (2.06 g, 70% yield based on DACO). − $C_{18}H_{24}N_4$·4HCl·H_2O (460.3): calcd. C 47.0, H 6.57, N 12.2; found C 46.8, H 6.81, N 11.8. − ^1H NMR (D_2O): δ = 1.82−1.88 (m, 4 H, $CH_2CH_2CH_2$), 3.18 (t, J = 5.7 Hz, 8 H, NCH_2CH_2), 4.30 (s, 4 H, CH_2-py), 7.84−8.66 (m, 8 H, py). − IR (KBr pellet): $\tilde{\nu}$ = 2986 cm^{-1} w, 2958 m, 1636 vs, 1617 s, 1541 s, 1468 s, 1443 s, 1390 vs, 930 m, 780 vs.

1-(Pyrid-2-ylmethyl)-1,5-diazacyclooctane Trihydrochloride Dihydrate (L^2·3HCl·$2H_2O$): A solution of DACO·2HBr (8.68 g, 31.7 mmol) and potassium hydroxide (3.30 g, 58.8 mmol) in anhydrous methanol (50 mL) was stirred for 4 h at room temperature. A solution of 2-(chloromethyl)pyridine hydrochloride (1.23 g, 7.5 mmol) in anhydrous ethanol was then added dropwise. The resulting mixture was refluxed for 1 h and then stirred at room temperature for ca. two days. The solvent was subsequently evaporated under reduced pressure, the residue was redissolved in water (20 mL), the pH of the resulting solution was adjusted to ca. 10 with Na_2CO_3, and then it was extracted with $CHCl_3$ (3 × 100 mL). The combined $CHCl_3$ extracts were dried, the solvent was evaporated, and the residue was purified by column chromatography on silica gel eluting with $CH_2Cl_2/MeOH/NH_3·H_2O$ (5:5:1). The free base, obtained as an oil, was dissolved in anhydrous ethanol; passage of HCl gas into this solution gave the salt as an off-white solid (1.7 g, 65% yield based on 2-(chloromethyl)pyridine hydrochloride used). − $C_{12}H_{19}N_3$·3HCl·$2H_2O$ (350.7): calcd. C 41.1, H 7.47, N 12.0; found C 40.8, H 7.69, N 11.8. − ^1H NMR (D_2O): δ = 1.90−1.96 (m, 4 H, $CH_2CH_2CH_2$), 3.02 (t, J = 5.7 Hz, 4 H, NCH_2CH_2), 3.24 (t, J = 5.9 Hz, 4 H, NCH_2CH_2), 4.15 (s, 2 H, CH_2-py), 7.77−8.42 (m, 4 H, py). − IR (KBr pellet): $\tilde{\nu}$ = 2953 cm^{-1} m, 1619 vs, 1546 m, 1466 s, 1406 w, 1327 w, 1230 m, 1073 m, 1038 w, 771 s.

Preparation of the Complexes: The mononuclear complex **1**, $[CuL^1Cl]ClO_4$, was prepared by mixing $Cu(ClO_4)_2·6H_2O$ (147 mg, 0.4 mmol) and L^1·4HCl·H_2O (184 mg, 0.4 mmol) in a 1:1 molar ratio in methanol/water solution. The pH of this solution was adjusted to ca. 6−7 with dilute aqueous NaOH solution. The resulting mixture was filtered and the filtrate was left to stand at room temperature. Blue single crystals suitable for X-ray analysis were obtained upon slow evaporation of the solvent. Yield: 119 mg (60%). − $C_{18}H_{24}Cl_2CuN_4O_4$ (494.9): calcd. C 43.7, H 4.89, N 11.1; found C 43.6, H 4.92, N 11.3. − FT-IR (KBr pellet): $\tilde{\nu}$ = 2952 cm^{-1} w, 2905 m, 1609 s, 1569 m, 1484 s, 1449 s, 1091 vs, 623 s. − Λ_M (methanol): 102 cm^2 Ω^{-1} mol^{-1}. − UV/vis: λ_{max}/nm (ε/dm^3 mol^{-1} cm^{-1}) (methanol): 622 (240), 260 (13300).

The dinuclear complex **2**, $[CuL^2Cl]_2(ClO_4)_2$, was obtained in a similar manner as described for the preparation of **1** (52%). − $C_{24}H_{38}Cl_4Cu_2N_6O_8$ (807.5): calcd. C 35.7, H 4.74, N 10.4; found C 35.4, H 4.88, N 10.3. − FT-IR (KBr pellet): $\tilde{\nu}$ = 2940 cm^{-1} w, 1610 s, 1573 m, 1481 m, 1454 s, 1082 vs, 1025 s, 621 s. − Λ_M (methanol): 184 cm^2 Ω^{-1} mol^{-1}. − UV/vis: λ_{max}/nm (ε/dm^3 mol^{-1} cm^{-1}) (methanol): 621 (330), 260 (17900).

$[CuL^1(N_3)]ClO_4$ (**3**), was synthesized by adding excess NaN_3 to a methanolic solution of **1**. The resulting mixture was filtered and the filtrate was left to stand at room temperature. Green single crystals suitable for X-ray analysis were obtained upon slow evaporation of the solvent (38%). − $C_{18}H_{24}ClCuN_7O_4$ (501.4): calcd. C 43.1, H 4.82, N 19.6; found C 42.9, H 4.98, N 19.3. − FT-IR (KBr pellet): $\tilde{\nu}$ = 2950 cm^{-1} m, 2125 s, 2031 vs, 1609 s, 1570 m, 1483 m, 1447 s, 1309 m, 1098 vs, 623 s. − Λ_M (methanol): 99 cm^2 Ω^{-1} mol^{-1}. − UV/vis: λ_{max}/nm (ε/dm^3 mol^{-1} cm^{-1}) (methanol): 618 (274), 263 (11200).

Magnetic Study: Variable-temperature magnetic susceptibility measurements on **2** were made on a SQUID magnetometer in the 5−300 K temperature range. The susceptibilities were corrected for diamagnetism using Pascal's constants for all the constituent atoms, and magnetic moments were calculated from the equation $\mu_{eff} = 2.828(\chi_M T)^{1/2}$.

Crystallographic Study: The reflection data were collected on an Enraf−Nonius CAD-4 X-ray diffractometer (for **1** and **2**) or a Bruker Smart 1000 CCD diffractometer (for **3**) equipped with a graphite crystal monochromator situated in the incident beam. The determination of unit cell parameters and data collections were performed with Mo-K_α radiation (λ = 0.71073 Å). Reflections in the range $4.5 \leq \theta \leq 25°$ (for **1** and **2**) and $1.71 \leq \theta \leq 25.03°$ (for **3**)

Table 4. Crystallographic data and structure refinement summary for **1**, **2**, and **3**

Complex	**1**	**2**	**3**
Empirical formula	$C_{18}H_{24}Cl_2CuN_4O_4$	$C_{24}H_{38}Cl_4Cu_2N_6O_8$	$C_{18}H_{24}ClCuN_7O_4$
M_r	494.86	807.50	501.43
Crystal size [mm^3]	0.25 × 0.30 × 0.30	0.20 × 0.30 × 0.55	0.15 × 0.30 × 0.40
Space group	$P2_1/n$	$P2_1/c$	$P2_1/n$
Temp. [K]	299(1)	299(1)	293(2)
a [Å]	7.824(2)	7.124(1)	15.5984(17)
b [Å]	22.562(5)	18.700(4)	7.5357(9)
c [Å]	11.840(2)	12.191(2)	17.799(2)
β [°]	94.50(3)	101.12(3)	91.648(2)
V [Å^3]	2084(1)	1594(1)	2091.3(4)
D [g cm^{-3}]	1.570	1.683	1.593
F(000)	1020	828	1036
Z	4	2	4
Unique reflections	2603	2086	3679
Observed reflections	1923	1763	3679
Parameters	262	199	280
R[a]	0.064	0.044	0.0316
R_w[b]	0.068	0.051	0.0827
S[c]	1.28	1.02	0.925
Largest diff. peak [e Å^{-3}]	0.51	0.73	0.294

[a] $R = \Sigma(||F_o| - |F_c||/\Sigma|F_o|)$. – [b] $Rw = [\Sigma w(|F_o| - |F_c|)^2/\Sigma wF_o{}^2]^{1/2}$, $w^{-1} = \sigma^2(F) + 0.0001F^2$ (for complexes **1** and **2**); $Rw = \{\Sigma[w(F_o{}^2 - F_c{}^2)^2]/\Sigma w(F_o{}^2)^2\}^{1/2}$, $w^{-1} = s^2(F_o{}^2) + (0.0554P)^2 + 0.7119P$, where $P = (F_o{}^2 + 2F_c{}^2)/3$ (for complex **3**). – [c] $S = \{\Sigma[w(F_o{}^2 - F_c{}^2)^2]/(n - p)\}^{1/2}$, where n = number of reflections measured and p = number of parameters used.

were collected at room temperature. All the structures were solved by direct methods and empirical absorption corrections were applied. Cu^{II} atoms in each complex were located from E-maps. All non-hydrogen atoms were determined by successive Fourier syntheses and were refined isotropically. The final refinement was performed by full-matrix least-squares methods against F (for **1** and **2**) or F^2 (for **3**) with anisotropic thermal parameters for non-hydrogen atoms. The hydrogen atoms were placed in theoretical positions as riding on the relevant atoms and were refined with fixed thermal factors. Crystallographic and refinement data for all three complexes are summarized in Table 4. Crystallographic data (excluding structure factors) for the structures reported in this paper have been deposited with the Cambridge Crystallographic Data Centre and allocated the deposition numbers CCDC-150458 (**1**), -150459 (**2**) and -150460 (**3**). Copies of the data may be obtained free of charge on application to the CCDC, 12 Union Road, Cambridge CB2 1EZ, U.K. [Fax: (internat). +44 (0)1223/336033; E-mail: deposit@ccdc.cam.ac.uk].

Acknowledgments

This work was financially supported by the National Natural Science Foundation of China (Grant Nos. 29771022 and 29971019), the Trans-Century Talents Training Program Foundation from the State Education Ministry of China, and the Natural Science Foundation of Tianjin, China.

---

[1] [1a] E. Kimura, T. Shiota, T. Koike, M. Shiro, M. Kodama, *J. Am. Chem. Soc.* **1990**, *112*, 5805–5811. – [1b] M. A. Halcrow, G. Christou, *Chem. Rev.* **1994**, *94*, 2421–2481 and references therein. – [1c]E. Kimura, T. Koike, M. Shionoya, *Metal Sites in Proteins and Models* (Eds.: H. A. O. Hill, P. Sadler, A. J. Thompson), *Structure and Bonding*, Vol. 89, Springer-Verlag, Berlin, Heidelberg, New York, **1997**, p 1. – [1d]K. P. Wainwright, *Coord. Chem. Rev.* **1997**, *166*, 35–90.

[2] W. K. Musker, *Coord. Chem. Rev.* **1992**, *117*, 133–157.

[3] [3a] J. I. Legg, D. O. Nielson, D. L. Smith, M. L. Larson, *J. Am. Chem. Soc.* **1968**, *90*, 5030–5031. – [3b] D. O. Nielson, M. L. Larson, R. D. Willett, J. I. Legg, *J. Am. Chem. Soc.* **1971**, *93*, 5079–5082. – [3c] D. K. Mills, J. H. Reibenspies, M. Y. Darensbourg, *Inorg. Chem.* **1990**, *29*, 4364–4366.

[4] [4a] X. H. Bu, Y. Y. Fang, Z. L. Shang, R. H. Zhang, *Acta Crystallogr., Sect. C* **1999**, *55*, 39–41. – [4b] X. H. Bu, Z. L. Shang, W. Weng, R. H. Zhang, H. P. Zhu, Q. T. Liu, *Acta Chem. Scand.* **1999**, *53*, 295–297. – [4c] X. H. Bu, M. Du, Z. L. Shang, R. H. Zhang, D. Z. Liao, M. Shionoya, T. Clifford, *Inorg. Chem.* **2000**, *39*, 4190–4199. – [4d] M. Du, Z. L. Shang, Q. Xu, R. H. Zhang, X. B. Leng, X. H. Bu, *Acta Crystallogr., Sect. C* **2000**, *56*, 769–770. – [4e] M. Du, L. H. Weng, X. B. Leng, X. H. Bu, R. H. Zhang, *Acta Crystallogr., Sect. C* **2000**, *56*, 1090–1091. – [4f] M. Du, X. H. Bu, X. B. Leng, Y. M. Guo, R. H. Zhang, *Acta Crystallogr., Sect. C* **2000**, *56*, 1314–1315.

[5] [5a] P. J. Farmer, T. Solouki, D. K. Mills, T. Soma, D. H. Russell, J. H. Reibenspies, M. Y. Darensbourg, *J. Am. Chem. Soc.* **1992**, *114*, 4601–4605. – [5b] R. M. Buonomo, I. Font, M. J. Maguire, J. H. Reibenspies, T. Tuntulani, M. Y. Darensbourg, *J. Am. Chem. Soc.* **1995**, *117*, 963–973. – [5c] G. Musie, C.-H. Lai, L. W. Sumner, M. Y. Darensbourg, *Inorg. Chem.* **1998**, *37*, 4086–4093.

[6] [6a] R. F. Drake, V. H. Crawford, N. W. Laney, W. E. Hatfield, *Inorg. Chem.* **1974**, *13*, 1246–1250. – [6b] W. E. Marsh, K. C. Patel, W. Hatfield, D. J. Hodgson, *Inorg. Chem.* **1983**, *22*, 511–515. – [6c] F. Tuna, L. Patron, Y. Journaux, M. Andruh, W. Plass, J.-C. Trombe, *J. Chem. Soc., Dalton Trans.* **1999**, 539–545. – [6d] M. Rodriguez, A. Llobet, M. Corbella, A. E. Martell, J. Reibenspies, *Inorg. Chem.* **1999**, *38*, 2328–2334.

[7] W. J. Geary, *Coord. Chem. Rev.* **1971**, *7*, 81–122.

[8] [8a] J. C. Colin, T. Mallah, Y. Journaux, F. Lloret, M. Julve, C. Bois, *Inorg. Chem.* **1996**, *35*, 4170–4176. – [8b] X. H. Bu, D. L. An, X. C. Cao, R. H. Zhang, T. Clifford, E. Kimura, *J. Chem. Soc., Dalton Trans.* **1998**, 2247–2252. – [8c] X. H. Bu, S. L. Lu, R. H. Zhang, D. Z. Liao, S. Aoki, T. Clifford, E. Kimura, *Inorg. Chim. Acta* **2000**, *298*, 50–56.

[9] C. O'Sullivan, G. Murphy, B. Murphy, B. Hathaway, *J. Chem. Soc., Dalton Trans.* **1999**, 1835–1844 and references therein.

[10] M. Brophy, G. Murphy, C. O'Sullivan, B. Hathaway, B. Murphy, *Polyhedron* **1999**, *18*, 611–615 and references therein.

[11] A. W. Addison, T. N. Rao, J. Reedijk, J. V. Rijn, G. C. Verschoor, *J. Chem. Soc., Dalton Trans.* **1984**, 1349–1356.

[12] G. R. Desiraju, *Acc. Chem. Res.* **1991**, *24*, 290−295.

[13] [13a] M. Munakata, L. P. Wu, M. Yamamoto, T. Kuroda-Sowa, M. Maekawa, *J. Am. Chem. Soc.* **1996**, *118*, 3117−3124. − [13b] T. Sugimori, N. Ohata, K. Koiwai, A. Odani, O. Yamauchi, *Inorg. Chem.* **1997**, *36*, 576−583.

[14] R. Haidar, M. Ipek, B. DasGupta, M. Yousaf, L. J. Zompa, *Inorg. Chem.* **1997**, *36*, 3125−3132.

[15] S. J. Brudenell, L. Spiccia, E. R. T. Tiekink, *Inorg. Chem.* **1996**, *35*, 1974−1979.

[16] G. A. McLachlan, G. D. Fallon, R. E. Martin, L. Spiccia, *Inorg. Chem.* **1995**, *34*, 254−261.

[17] [17a] T. Szabo-Planka, A. Rockenbauer, M. Gyor, F. Gaizer, *J. Coord. Chem.* **1988**, *17*, 69−83. − [17b] M. Murali, M. Palaniandavar, T. Pandiyan, *Inorg. Chim. Acta* **1994**, *224*, 19−25.

[18] K. Miyoshi, H. Tanaka, E. Kimura, S. Tsuboyama, S. Murata, H. Shimizu, K. Ishizu, *Inorg. Chim. Acta* **1983**, *78*, 23−30.

[19] I. Bertini, G. Canti, R. Grassi, A. Scazzofola, *Inorg. Chem.* **1980**, *19*, 2198−2200.

[20] R. Lucas, S. Liu, L. K. Thompson, *Inorg. Chem.* **1990**, *29*, 85−88.

[21] Y. Journaux, J. Sletten, O. Kahn, *Inorg. Chem.* **1985**, *24*, 4063−4069.

[22] W. E. Marsh, W. E. Hatfield, D. J. Hodson, *Inorg. Chem.* **1982**, *21*, 2679−2684.

[23] W. E. Marsh, W. E. Hatfield, D. J. Hodson, *Inorg. Chem.* **1988**, *27*, 1819−1822.

[24] [24a] J. F. Villa, W. Hatfield, *Inorg. Chem.* **1971**, *11*, 1331−1334. − [24b] D. M. Duggan, D. N. Hendrickson, *Inorg. Chem.* **1974**, *13*, 2929−2940.

[25] O. Kahn, S. Sikorav, J. Gouteron, S. Jeannin, *Inorg. Chem.* **1983**, *22*, 2877−2883.

[26] D. D. Swank, G. F. Needham, R. D. Willett, *Inorg. Chem.* **1979**, *18*, 761−765.

[27] E. D. Estes, W. E. Estes, W. E. Hatfield, D. J. Hodgson, *Inorg. Chem.* **1975**, *14*, 106−109.

[28] D. Y. Jeter, D. J. Hodgson, W. E. Hatfield, *Inorg. Chim. Acta* **1971**, *5*, 257−259.

[29] E. L. Buhle, A. M. Moore, F. G. Wiseloge, *J. Am. Chem. Soc.* **1943**, *65*, 29−32.

[30] J. H. Billman, L. C. Dorman, *J. Org. Chem.* **1962**, *27*, 2419−2422.

Received October 7, 2000
[I00374]